Inorganic Chemistry
Article

Inorg. Chem. **2010**, *49*, 4125–4132 **4125**
DOI: 10.1021/ic9024712

A New Family of Sandwich-Type Polytungstophosphates Containing Two Types of Metals in the Central Belt: $M'_2M_2(PW_9O_{34})_2^{12-}$ (M′ = Na or Li, M = Mn^{2+}, Co^{2+}, Ni^{2+}, and Zn^{2+})

Yu Hou,[†] Lin Xu,[‡] Morgan J. Cichon,[†] Sheri Lense,[†] Kenneth I. Hardcastle,[†] and Craig L. Hill*[,†]

[†]*Department of Chemistry, Emory University, 1515 Dickey Drive, Atlanta, Georgia 30322 , and* [‡]*Institute of Polyoxometalates, Department of Chemistry, Northeast Normal University, Renmin Street 5268, Changchun 130024 People's Republic of China*

Received December 13, 2009

A new family of sandwich-type polytungstophosphates containing two different types of metals in the central belt, $M'_2M_2(PW_9O_{34})_2^{12-}$ (M′ = Na or Li, M = Mn^{2+}, Co^{2+}, Ni^{2+}, and Zn^{2+}), have been synthesized and characterized by infrared spectroscopy, ^{31}P solution NMR spectroscopy, and elemental analysis. Compounds $Na_2Co_2(PW_9O_{34})_2^{12-}$ (**Na2Co2**), $Na_2Ni_2(PW_9O_{34})_2^{12-}$ (**Na2Ni2**), $Li_2Ni_2(PW_9O_{34})_2^{12-}$ (**Li2Ni2**), $Na_2Mn_2(PW_9O_{34})_2^{12-}$ (**Na2Mn2**), and $Li_2Zn_2(PW_9O_{34})_2^{12-}$ (**Li2Zn2**) were characterized by X-ray crystallography. All these compounds have similar structures, in which two transition-metal ions and two alkali metal ions (sodium or lithium) are sandwiched between two [B-α-PW_9O_{34}]$^{9-}$ units; the transition and alkali metals reside in the internal and external (solvent exposed) positions of the central belt, respectively. By adding LiCl to aqueous solutions of compounds **Na2M2**, lithium−sodium exchanges in the external belt positions are observed by ^{31}P solution NMR spectroscopy and X-ray crystallography. Magnetic measurements indicate ferromagnetic exchange interactions between the two Ni^{2+} ions in **Na2Ni2** at 10−300 K and the two Co^{2+} ions in **Na2Co2** at 6−30 K. In contrast, **Na2Mn2** exhibits an antiferromagnetic interaction between the Mn^{2+} ions at 2−50 K.

Introduction

Polyoxometalates (POMs) and transition-metal-containing POMs (d^0 POMs binding one or more d-electron metals) are large classes of highly modifiable discrete metal−oxygen anionic clusters[1] with substantial structural diversity and with widely ranging properties facilitating applications in medicine,[2] catalysis,[3] and magnetism.[4] Within the family of transition-metal-containing POMs, sandwich-type compounds (one or more transition metals bonded between two POM lacunary fragments) represent the largest subclass.[5] They have been referred to as oxidatively stable inorganic analogues of metalloporphyrins and used as catalysts for a range of organic oxidations.[6]

*Corresponding author. Fax: (+1) 404-727-6076. E-mail: chill@emory.edu.

(1) (a) Pope, M. T. *Heteropoly and Isopoly Oxometalates*; Springer-Verlag: Berlin, Germany, 1983. (b) Pope, M. T.; Müller, A. *Angew. Chem., Int. Ed. Engl.* **1991**, *30*, 34. (c) Hill, C. L. *Chem. Rev.* **1998**, *98*, special thematic issue. (d) *Polyoxometalate Chemistry: From Topology Via Self-Assembly to Applications*; Pope, M. T., Müller, A., Eds.; Kluwer: Dordrecht, The Netherlands, 2001. (e) *Polyoxometalate Chemistry for Nanocomposite Design*; Pope, M. T., Yamase, T., Eds.; Kluwer: Dordrecht, The Netherlands, 2002. (f) *Polyoxometalate Molecular Science*; Borrás-Almenar, J. J., Coronado, E., Müller, A., Pope, M. T., Eds.; Kluwer: Dordrecht, The Netherlands, 2003. (g) Pope, M. T. In *Comprehensive Coordination Chemistry II*; McCleverty, J. A., Meyer, T. J., Eds.; Elsevier Ltd.: Oxford, U.K., 2004; Vol. *4*, p 635. (h) Cronin, L. In *Comprehensive Coordination Chemistry II*; McCleverty, J. A., Meyer, T. J., Eds.; Elsevier Ltd.: Oxford, U.K., 2004; Vol. *7*, p 1. (i) Hill, C. L. In *Comprehensive Coordination Chemistry II*; Wedd, A. G., Ed.; Elsevier Ltd.: Oxford, U.K., 2004; Vol. *4*, p 679.

(2) (a) *Polyoxometalates: From Platonic Solids to Anti-retroviral Activity*; Pope, M. T., Müller, A., Eds.; Kluwer: Dordrecht, Netherlands, 1993. (b) Yamase, T.; Fujita, H.; Fukushima, K. *Inorg. Chim. Acta* **1988**, *151*, 15. (c) Hill, C. L.; Weeks, M.; Hartnup, M.; Sommadossi, J.-P.; Schinazi, R. *Ann. N.Y. Acad. Sci.* **1990**, *616*, 528. (d) Hill, C. L.; Weeks, M.; Schinazi, R. F. *J. Med. Chem.* **1990**, *33*, 2767. (e) Yamase, T. In *Polymeric Materials Encyclopedia*, Salamone, J. C., Ed; CRC Press: Boca Raton, FL, 1996; p 365. (f) Rhule, J. T.; Hill, C. L.; Judd, D. A.; Schinazi, R. F. *Chem. Rev.* **1998**, *98*, 327. (g) Rhule, J. T.; Hill, C. L.; Zheng, Z.; Schinazi, R. F. Metallopharmaceuticals. In *Topics in Biological Inorganic Chemistry*, Clarke, M. J., Sadler, P. J., Eds.; Springer-Verlag, Heidelberg, Germany, 1999; Vol. *2*, p 117. (h) Seko, A.; Yamase, T.; Yamashita, K. *J. Inorg. Biochem.* **2009**, *103*(7), 1061. (i) Prudent, R.; Moucadel, V.; Laudet, B.; Barette, C.; Lafanechere, L.; Hasenknopf, B.; Li, J.; Bareyt, S.; Lacote, E.; Thorimbert, S.; Malacria, M.; Gouzerh, P.; Cochet, C. *Chem. & Bio.* **2008**, *15*(7), 683. (j) Mueller, C. E.; Iqbal, J.; Baqi, Y.; Zimmermann, H.; Roellich, A.; Stephan, H. *Bioorg. Med. Chem. Lett.* **2006**, *16*(23), 5943.

(3) (a) Hill, C. L. *J. Mol. Catal. A: Chem.* **2007**, *262*(1−2), 2. (b) Hill, C. L.; Prosser-McCartha, C. M. *Coord. Chem. Rev.* **1995**, *143*, 407. (c) Alhanash, A.; Kozhevnikova, E. F.; Kozhevnikov, I. V. *Catal. Lett.* **2008**, *120*(3−4), 307. (d) Moffat, J. B. *Metal-Oxygen Clusters: The Surface and Catalytic Properties of Heteropoly Oxometalates.* Kluwer Academic/Plenum Publishers: New York, 2001; Vol. *9*, p 308. (e) Kozhevnikov, I. V.; Wiley, Chichester, England, 2002; p 216. (f) Okuhara, T.; Mizuno, N.; Misono, M. *Adv. Catal.* **1996**, *41*, 113. (g) Katsoulis, D. E. *Chem. Rev.* **1998**, *98*, 359. (h) Mizuno, N.; Misono, M. *Chem. Rev.* **1998**, *98*, 199. (i) Kozhevnikov, I. V. *Chem. Rev.* **1998**, *98*, 171. (j) Neumann, R. *Prog. Inorg. Chem.* **1998**, *47*, 317. (k) Müller, A.; Das, S. K.; Kuhlmann, C.; Bógge, H.; Schmidtmann, M.; Diemann, E.; Krickemeyer, E.; Hormes, J.; Modrow, H.; Schindler, M. *Chem. Commun.* **2001**, 655.

Published on Web 04/01/2010

Trivacant Keggin and Wells−Dawson lacunary POMs have been extensively used as precursors to prepare sandwich-type POMs because replacement of several adjacent high-valent tungsten centers with low-valent metals modifies the surface properties of metal-oxide-like structural units.[7] Trivacant POMs are classified as A-type (removal of one corner-sharing MO_6 octahedron from each of three adjacent M_3O_{13} triads) and B-type (removal of one entire M_3O_{13} triad).[7c]

Reactions of A-type tricavant POMs and transition or main-group metals commonly form structures with a single substituted POM unit, such as those with the formula $[A\text{-}M_3(H_2O)_3XW_9O_{37}]^{n-}$ (X = Si^{IV}, Ge^{IV}; M = Al^{3+}, Ga^{3+}, In^{3+}, Cr^{3+}, V^{3+}, Fe^{3+}, Mn^{2+}, Co^{2+}, Ni^{2+}, Cu^{2+};[7a,b,8a−h] X = P^V; M_3 = $Fe_{3-x}Ni_x$[8c,e]) or those with a sandwich type structure, such as $[M_3(H_2O)_3(A\text{-}XW_9O_{34})_2]^{n-}$ (X = P^V, Si^{IV}; M = Sn^{2+}, Co^{2+}, Mn^{2+}, Ni^{2+}, Cu^{2+}, Zn^{2+}, Fe^{3+} Pd^{2+}), $[(CeO)_3(H_2O)_2(A\text{-}PW_9O_{34})_2]^{12-}$, and $[(ZrOH)_3(A\text{-}SiW_9O_{34})_2]^{11-}$.[9]

Among the POMs based on $[B\text{-}\alpha\text{-}XW_9O_{34}]^{n-}$ and $[B\text{-}\alpha\text{-}X_2W_{15}O_{56}]^{n-}$ polyanions, those with three or four transition metals in the structures are widely documented, including the following: $[M_3(H_2O)_3(\alpha\text{-}XW_9O_{33})_2]^{n-}$ (X = As^{III}, Sb^{III}, Se^{IV}, Te^{IV}; M = Mn^{2+}, Co^{2+}, Ni^{2+}, Cu^{2+}, Zn^{2+}); $[(VO)_3(\alpha\text{-}XW_9O_{33})_2]^{n-}$ (X = As^{III}, Sb^{III}, Bi^{III});[10] $[M_3P_2W_{15}O_{62}]^{n-}$ (M = Ti^{4+}, Zr^{4+}, Hf^{4+}, V^{5+}, Nb^{5+}, Ta^{5+}, Mo^{6+});[1a,11,12] $[(NaOH_2)Co_3(H_2O)(P_2W_{15}O_{56})_2]^{17\text{-}6d}$ $[\alpha\alpha\beta\alpha\text{-}(NaOH_2)(Fe^{III}OH_2)Fe^{III}{}_2(P_2W_{15}O_{56})_2]^{14-}$;[7c] $[Ni_3Na(H_2O)_2(XW_9O_{34})_2]^{11-}$ (X = P^V, As^V);[13] $[M_4(H_2O)_2(XW_9O_{34})_2]^{n-}$ (X = P^V, Si^{IV}, Ge^{IV}; M = Mn^{2+}, Co^{2+}, Zn^{2+}, Co^{2+}, Ni^{2+});[14] and $[M_4(H_2O)_2(X_2W_{15}O_{56})_2]^{n-}$ (X = P^V, As^V; M = Mn^{2+}, Co^{2+}, Ni^{2+}, Cu^{2+}, Zn^{2+}, Cd^{2+}, Fe^{3+}).[15]

While many sandwich-type POMs containing three or four transition metals in the central belt based on Keggin or Wells−Dawson fragments have been documented, very few of the corresponding derivatives with two transition metals in the belt are known. The Hill group reported X-ray crystal structures of Wells−Dawson derivatives containing two transition metals in the central belt $[(NaOH_2)_2M_2(X_2W_{15}O_{56})_2]^{n-}$ (X = P^V, M = Fe^{3+}, Cu^{2+}; X = As^V, M = Fe^{3+}),[16,7c] and subsequently, Ruhlmann and Thouvenot's group reported the Co^{2+} analogue whose structure was confirmed by IR, elemental analysis, and ^{31}P solution NMR spectroscopy.[6d] In addition, diuranium and dineptunium containing POMs have also been obtained based on an A-type trivacant Keggin unit, including $[M_2(UO_2)_2(A\text{-}XW_9O_{34})_2]^{n-}$ (X = P^V, M = K, Na, NH_4; X = Ge^{IV}, Si^{IV}; M = Na), $[(UO_2)_2(H_2O)_2(XW_9O_{33})_2]^{n-}$ (X = Sb^{III}, Te^{IV}),[17] and $[Na_2(NpO_2)_2(A\text{-}PW_9O_{34})_2]^{14-}$.[18] However, sandwich-type polyoxoanions with two transition metals in the central belt based on the $[B\text{-}\alpha\text{-}PW_9O_{34}]^{9-}$ Keggin fragment are, to our knowledge, unknown.

(4) (a) Coronado, E.; Gómez-García, C. J. In *Polyoxometallates: From Platonic Solids to Anti-Retroviral Activity*; Pope, M. T., Müller, A., Eds.; Kluwer Academic Publishers: Norwell, MA, 1994; p 233. (b) Coronado, E.; Gómez-García, C. J. *Chem. Rev.* **1998**, *98*, 273. (c) Clemente-Juan, J. M.; Coronado, E. *Coord. Chem. Rev.* **1999**, *193−195*, 361. (d) Clemente-Juan, J. M.; Clemente-León, M.; Coronado, E.; Forment, A.; Gaita-Ariño, A.; Gómez-García, C. J.; Martínez-Ferrero, E. In *Polyoxometalate Chemistry for Nanocomposite Design*; Yamase, T., Pope, M. T., Eds.; Kluwer Academic/Plenum Publishers: Norewell, MA, 2002; p 157. (e) Clemente-Juan, J. M. M.; Coronado, E.; Forment, A.; Gaita-Ariño, A. In *Polyoxometalate Molecular Science, NATO Science series*; Borrás-Alamenar, J. J., Coronado, E., Müller, A., Pope, M. T., Eds.; Kluwer Academic Publishers: Norwell, MA, 2003; p 273. (f) Ouahab, L.; Golhen, S.; Triki, S. *Polyoxometalate Chemistry* **2001**, 205.

(5) Bi, L.; Kortz, U.; Keita, B.; Nadjo, L.; Borrmann, H. *Inorg. Chem.* **2004**, *43*, 8367.

(6) (a) Hill, C. L.; Brown, R. B. *J. Am. Chem. Soc.* **1986**, *108*, 536–538. (b) Lyon, D. K.; Miller, W. K.; Novet, T.; Domaille, P. J.; Evitt, E.; Johnson, D. C.; Finke, R. G. *J. Am. Chem. Soc.* **1991**, *113*, 7209. (c) Mansuy, D.; Bartoli, J. F.; Lyon, D. K.; Finke, R. G. *J. Am. Chem. Soc.* **1991**, *113*, 7222. (d) Ruhlmann, L.; Canny, J.; Contant, R.; Thouvenot, R. *Inorg. Chem.* **2002**, *41*, 3811.

(7) (a) Katsoulis, D. E.; Pope, M. T. *J. Am. Chem. Soc.* **1984**, *106*, 2737. (b) Liu, J. G.; Ortega, F.; Sethuraman, P.; Katsoulis, D. E.; Costello, C. E.; Pope, M. T. *J. Chem. Soc., Dalton Trans.* **1992**, 1901. (c) Anderson, T. M.; Zhang, X.; Hardcastle, K. I.; Hill, C. L. *Inorg. Chem.* **2002**, *41*, 2477.

(8) (a) Liu, J. F.; Zhao, B. L.; Rong, C. Y.; Pope, M. T. *Acta Chim. Sin. (Engl. Ed.)* **1993**, *51*, 368. (b) Qu, L. Y.; Sun, Y. J.; Chen, Y. G.; Yu, M.; Peng, J. *Synth. React. Inorg. Met.-Org. Chem.* **1994**, *24*, 1339. (c) Mizuno, N.; Hirose, T.; Tateishi, M.; Iwamoto, M. *J. Mol. Catal.* **1994**, *88*, L125–L131. (d) Meng, L.; Liu, J. F.; Wu, Y.; Xiao, Y.; Zhao, D. *Chin. J. Chem.* **1995**, *13*, 334. (e) Mizuno, N.; Nozaki, C.; Hirose, T.; Tateishi, M.; Iwamoto, M. *J. Mol. Catal. A: Chem.* **1997**, *117*(1−3), 159. (f) Liu, J. F.; Zhen, Y. G.; So, H. S. *Synth. React. Inorg. Met.-Org. Chem.* **1998**, *28*, 863. (g) Meng, L.; Zhan, X. P.; Wang, M.; Liu, J. F. *Polyhedron* **2001**, *20*, 881. (h) Jana, S. K.; Kubota, Y.; Tatsumi, T. *J. Catal.* **2008**, *255*(1), 40.

(9) (a) Knoth, W. H.; Domaille, P. J.; Farlee, R. D. *Organometallics* **1985**, *4*, 62. (b) Knoth, W. H.; Domaille, P. J.; Harlow, R. L. *Inorg. Chem.* **1986**, *25*, 1577. (c) Finke, R. G.; Rapko, B.; Weakley, T. J. R. *Inorg. Chem.* **1989**, *28*, 1573. (d) Xin, F.; Pope, M. T. *J. Am. Chem. Soc.* **1996**, *118*, 7731. (e) Laronze, N.; Marrot, J.; Hervé, G. *Inorg. Chem.* **2003**, *42*, 5857.

(10) (a) Robert, F.; Leyrie, M.; Hervé, G. *Acta Crystallogr.* **1982**, *B38*, 358. (b) Bösing, M.; Nöh, A.; Loose, I.; Krebs, B. *J. Am. Chem. Soc.* **1998**, *120*, 7252. (c) Kortz, U.; Al-Kassem, N. K.; Savelieff, M. G.; Al Kadi, N. A.; Sadakane, M. *Inorg. Chem.* **2001**, *40*, 4742. (d) Botar, B.; Yamase, T.; Ishikawa, E. *Inorg. Chem. Commun.* **2001**, *4*, 551. (e) Yamase, T.; Botar, B.; Ishikawa, E.; Fukaya, K. *Chem. Lett.* **2001**, 56. (f) Mialane, P.; Marrot, J.; Riviére, E.; Nebout, J.; Hervé, G. *Inorg. Chem.* **2001**, *40*, 44. (g) Kortz, U.; Nellutla, S.; Stowe, A. C.; Dalal, N. S.; van Tol, J.; Bassil, B. S. *Inorg. Chem.* **2004**, *43*, 144.

(11) Finke, R. G.; Rapko, B.; Saxton, R. J.; Domaille, P. J. *J. Am. Chem. Soc.* **1986**, *108*, 2947.

(12) Meng, L.; Liu, J. F. *Chin. Chem. Lett.* **1994**, *6*, 547.

(13) (a) Kortz, U.; Mbomekalle, I. M.; Keita, B.; Nadjo, L.; Berthet, P. *Inorg. Chem.* **2002**, *41*, 6412. (b) Mbomekalle, I. M.; Keita, B.; Nadjo, L.; Berthet, P. *Inorg. Chem. Commun.* **2003**, *6*, 435.

(14) (a) Weakley, T. J. R.; Evans, H. T., Jr; Showell, J. S.; Tourné, G. F.; Tourné, C. M. *J. Chem. Soc. Chem. Commun.* **1973**, 139. (b) Casañ-Pastor, N.; Bas-Serra, J.; Coronado, E.; Pourroy, G. L.; Baker, L. C. W. *J. Am. Chem. Soc.* **1992**, *114*, 10380. (c) Clemete-Juan, J. M.; Coronado, E.; Galán-Mascarós, J. R.; Gómez-García, C. J. *Inorg. Chem.* **1999**, *38*, 55. (d) Kortz, U.; Isber, S.; Dickman, M. H.; Ravot, D. *Inorg. Chem.* **2000**, *39*, 2915. (e) Kortz, U.; Nellutla, S.; Stowe, A. C.; Dalal, N. S.; Rauwald, U.; Danquah, W.; Ravot, D. *Inorg. Chem.* **2004**, *43*, 2308. (f) Bassil, B. S.; Dickman, M. H.; Kortz, U. *Inorg. Chem.* **2006**, *45*, 2394.

(15) (a) Finke, R. G.; Droege, M. W. *Inorg. Chem.* **1983**, *22*, 1006. (b) Finke, R. G.; Droege, M. W.; Domaille, P. J. *Inorg. Chem.* **1987**, *26*, 3886. (c) Weakley, T. J. R.; Finke, R. G. *Inorg. Chem.* **1990**, *29*, 1235. (d) Gómez-García, C. J.; Borrás-Almenar, J. J.; Coronado, E.; Ouahab, L. *Inorg. Chem.* **1994**, *33*, 4016. (e) Finke, R. G.; Weakley, T. J. R. *J. Chem. Crystallogr.* **1994**, *24*, 123. (f) Kirby, J. F.; Baker, L. C. W. *J. Am. Chem. Soc.* **1995**, *117*, 10010. (g) Crano, N. J.; Chambers, R. C.; Lunch, V. M.; Fox, M. A. *J. Mol. Catal. A: Chem.* **1996**, *114*, 65. (h) Zhang, X.; Duncan, D. C.; Campana, C. F.; Hill, C. L. *Inorg. Chem.* **1997**, *36*, 4208. (i) Müller, A.; Peter, F.; Pope, M. T.; Gatteschi, D. *Chem. Rev.* **1998**, *98*, 239. (j) Song, W.; Wang, X.; Liu, Y.; Liu, J.; Xu, H. *J. Electroanal. Chem.* **1999**, *479*, 85. (k) Gaunt, A. J.; May, I.; Collison, D.; Holman, K. T.; Pope, M. T. *J. Mol. Struct.* **2003**, *656*, 101.

(16) (a) Zhang, X.; Hill, C. L. *Chem. Ind.* **1998**, *75*, 519. (b) Anderson, T. M.; Hardcastle, K. I.; Okun, N.; Hill, C. L. *Inorg. Chem.* **2001**, *40*, 6418. (c) Zhang, X.; Anderson, T. M.; Chen, Q.; Hill, C. L. *Inorg. Chem.* **2001**, *40*, 418. (d) Mbomekalle, I. M.; Keita, B.; Nadjo, L.; Neiwert, W. A.; Zhang, L.; Hardcastle, K. I.; Hill, C. L.; Anderson, T. M. *Eur. J. Inorg. Chem.* **2003**, 3924. (e) Keita, B.; Mbomekalle, I. M.; Lu, Y. W.; Nadjo, L.; Berthet, P.; Anderson, T. M.; Hill, C. L. *Eur. J. Inorg. Chem.* **2004**, 3462.

(17) (a) Kim, K.-C.; Pope, M. T. *J. Am. Chem. Soc.* **1999**, *121*, 8512. (b) Kim, K.-C.; Gaunt, A. J.; Pope, M. T. *J. Cluster Sci.* **2002**, *13*, 423. (c) Gaunt, A. J.; May, I.; Copping, R.; Bhatt, A. I.; Collison, D.; Danny-Fox, O.; Travis-Holman, K.; Pope, M. T. *J. Chem. Soc., Dalton Trans.* **2003**, 3009. (d) Khoshnavazi, R.; Eshtiagh-hossieni, H.; Alizadeh, M. H.; Pope, M. T. *Polyhedron* **2006**, *25*, 1921. (e) Tan, R.; Wang, X.; Chai, F.; Lan, Y.; Su, Z. *Inorg. Chem. Commun.* **2006**, *9*(12), 1331.

(18) Gaunt, A. J.; May, I.; Helliwell, M.; Richardson, S. *J. Am. Chem. Soc.* **2002**, *124*, 13350.

We report here the syntheses, structures, and magnetic properties of a new family of sandwich-type polyoxoanions, $[M'_2M_2(PW_9O_{34})_2]^{12-}$, (M′ = Na or Li, M = Mn^{2+}, Co^{2+}, Ni^{2+}, Zn^{2+}) in which two [B-α-PW_9O_{34}]$^{9-}$ units sandwich two metal ions in the internal positions of the central belt and two sodium or lithium ions in the exterior positions of this belt.

Experimental Section

General Methods and Materials. All common laboratory chemicals were reagent grade, purchased from commercial sources, and used without further purification. Elemental analyses for Li, Na, K, P, Co, Ni, Mn, Zn, and W were performed by Desert Analytics, now Columbia (Tucson, Arizona), and by Galbraith Laboratories, Inc. (Knoxville, Tennessee). Elemental analyses for H were performed by Atlantic microlab (Norcross, GA). Infrared spectra (2% sample in KBr) were recorded on a Nicolet 510 instrument. The kinetics were studied using an Agilent 8453 spectrophotomer. Solution ^{31}P NMR spectra were obtained on Unity Plus 600 (277, 286, and 296 K) or Varian INOVA 400 spectrometers (296 K) and referenced to 85% H_3PO_4 (0.0 ppm) external standard. The numbers of counter cations were determined by elemental analysis. The magnetic susceptibility measurements were carried out on polycrystalline samples using a Quantum Design MPMS-XL5 SQUID magnetometer at 1000 Oe in the temperature range 2−300 K. Diamagnetic corrections were estimated from Pascal's constants.

$K_8Na_4[Na_2Co_2(PW_9O_{34})_2]\cdot 28H_2O$ (Na2Co2). $Na_2WO_4\cdot 2H_2O$ (5 g, 15.2 mmol) and Na_2HPO_4 (0.24, 1.7 mmol) were dissolved in 100 mL H_2O followed by an addition of $Co(NO_3)_2\cdot 6H_2O$ (0.31 g, 1.1 mmol), resulting in a cloudy suspension. The pH was adjusted to 7.5 by dropwise addition of 6 M HCl, and a purple solution formed. The solution was heated at 90 °C for 1 h and then was allowed to cool to room temperature. Powdered KCl (0.6 g, 8.0 mmol) was added, and the solution was left to slowly evaporate at room temperature. After several days, purple needle crystals suitable for X-ray diffraction were formed (yield 0.2 g, 7% based on W). Reheating and evaporation of the filtrate can increase the yield (up to 20%). FTIR data (cm^{-1}): 1057(s), 1019(s), 970(sh), 954(sh), 934(s), 904(m), 865(m), 801(s), 734(s). Elemental analysis calcd (%) for **Na2Co2**: K, 5.6; Na, 2.5; P, 1.1; W, 59.8; Co, 2.1. Found (%): K, 5.8; Na, 2.4; P, 1.2; W, 59.6; Co, 2.0.

$K_8Na_4[Na_2Ni_2(PW_9O_{34})_2]\cdot 30H_2O$ (Na2Ni2). The synthetic procedure was similar to that of **Na2Co2** but using $Ni(NO_3)_2\cdot 6H_2O$ (0.31 g, 1.1 mmol) in place of $Co(NO_3)_2\cdot 6H_2O$. After several days, yellow-green needle crystals suitable for X-ray diffraction were formed (yield 0.3 g, 10% based on W). Reheating and evaporation of the filtrate can increase the yield up to 23%. FTIR data (cm^{-1}): 1041(s), 1021(s), 968(sh), 955(sh), 933(m), 922(m), 908(m), 872(m), 805(s), 737(s). Elemental analysis calcd (%) for **Na2Ni2**: K, 5.6; Na, 2.5; P, 1.1; W, 59.5; Ni, 2.1. Found (%): K, 5.9; Na, 2.7; P, 1.1; W, 60.0; Ni, 2.0.

$Na_{12}[Na_2Mn_2(PW_9O_{34})_2]\cdot 36H_2O$ (Na2Mn2). The synthetic procedure was similar to that of **Na2Co2**, but $Mn(CH_3COO)_2\cdot 4H_2O$ (0.266 g, 1.1 mmol) was used instead of the cobalt(II) precursor. After several days, yellow crystals suitable for X-ray diffraction were formed (yield 0.3 g, 10% based on W). FTIR data (cm^{-1}): 1057(s), 1019(s), 965(sh), 957(sh), 937(s), 893(s), 861(m), 810(s), 740(s). Elemental analysis calcd (%) for **Na2Mn2**: Na, 6.1; P, 1.2; W, 62.4; Mn, 2.1. Found (%): Na, 5.9; P, 1.1; W, 61.1; Mn, 2.1.

$K_8Na_4[Na_2Zn_2(PW_9O_{34})_2]\cdot 31H_2O$ (Na2Zn2). The synthetic procedure was similar to the preparation of **Na2Co2**, but $Zn(NO_3)_2\cdot 6H_2O$ (0.31 g, 1.1 mmol) was used. After heating the reaction solution at 90 °C for 1 h, a very small quantity of precipitate formed which was removed by filtration, and 0.5 g KCl was then added. The solution was left to slowly evaporate at room temperature until colorless crystals were obtained (yield 0.5 g, 15% based on W). FTIR data (cm^{-1}): 1051(s), 1016(s), 968(sh), 956(sh), 935(s), 921(s), 906(m), 869(sh), 805(s), 735(s). Elemental analysis calcd (%) for **Na2Zn2**: K, 5.7; Na, 2.5; P, 1.1; W, 60.1; Zn, 2.3. Found (%): K, 5.5; Na, 2.7; P, 1.2; W, 59.2; Zn, 2.1.

$K_6Li_6[Li_2Co_2(PW_9O_{34})_2]\cdot 38H_2O$ (Li2Co2). Na2Co2 (1.3 g) was dissolved in minimal amount of 1 M LiCl solution. Purple crystals were obtained after several days upon slow evaporation (yield 0.7 g, 54% based on W). FTIR data (cm^{-1}): 1056(s), 1028(s), 969(sh), 958(sh), 940(s), 899(s), 866(sh), 800(s), 742(s). Elemental analysis calcd (%) for **Li2Co2**: Li, 1.0; K, 4.2; P, 1.1; W, 59.6; Co, 2.1. Found (%): Li, 0.9; K, 4.2; P, 1.0; W, 58.6; Co, 2.0.

$K_6Li_6[Li_2Ni_2(PW_9O_{34})_2]\cdot 28H_2O$ (Li2Ni2). Na2Ni2 (1.0 g) was dissolved in a minimal amount of 1 M LiCl solution. Single crystals suitable for X-ray crystallography were obtained after several days upon slow evaporation (yield 0.44 g, 44% based on W). FTIR data (cm^{-1}): 1041(s), 1033(s), 974(sh), 959(sh), 943(m), 920(sh), 904(m), 872(sh), 796(sh), 743(s). Elemental analysis calcd (%) for **Li2Ni2**: K, 4.4; Li, 1.0; P, 1.2; W, 61.7; Ni, 2.2. Found (%): K, 4.5; Li, 1.0; P, 1.1; W, 59.9; Ni, 2.0.

$K_3Na_3Li_6[Li_2Mn_2(PW_9O_{34})_2]\cdot 40H_2O$ (Li2Mn2). Na2Mn2 (1.5 g) was dissolved in a minimal amount of 1 M LiCl solution. Yellow crystals were obtained after several days upon slow evaporation (yield 0.42 g, 27% based on W). FTIR data (cm^{-1}): 1058(s), 1024(s), 971(sh), 957(sh), 939(s), 893(s), 861(w), 797(m), 741(s). Elemental analysis calcd (%) for **Li2Mn2**: Li, 1.0; K, 2.1; P, 1.1; W, 59.8; Mn, 2.0. Found (%): Li, 1.0; K, 1.9; P, 1.0; W, 58.2; Mn, 1.9.

$K_6Na_2Li_4[Li_2Zn_2(PW_9O_{34})_2]\cdot 25H_2O$ (Li2Zn2). Na2Zn2 (0.8 g) was dissolved in a minimal amount of 1 M LiCl solution. Single crystals suitable for X-ray crystallography were obtained after several days upon slow evaporation (yield 0.31 g, 38% based on W). FTIR data (cm^{-1}): 1052(s), 1025(s), 971(sh), 958(sh), 939(s), 903(m), 867(sh), 793(m), 743(s). Elemental analysis calcd (%) for **Li2Zn2**: K, 4.4; Na, 0.9; P, 1.2; W, 61.8; Zn, 2.4. Found (%): K, 4.2; Na, 0.7; P, 1.1; W, 59.0; Zn, 2.2.

Lithium−sodium Exchange Experiments. Typically, about 15 mg of **Na2Co2** or **Na2Ni2** was added to 700 μL of a D_2O solution in a 5 mm i.d. NMR tube, and the spectrum recorded quickly. Compounds **Na2Co2** and **Na2Ni2** did not dissolve completely, so the exact concentration of **Na2Co2** or **Na2Ni2** in the lithium−sodium exchange experiments in these cases was not attainable. In the indicated cases, 10 μL of 0.2 M LiCl D_2O solution was added (the resulting concentration of LiCl is 2.8 mM), and the NMR spectra were recorded as a function of time. These experiments were conducted at three different temperatures: 277, 286, and 296 K.

Single X-ray Crystallography. The complete data sets for **Na2Co2**, **Na2Ni2**, **Li2Ni2**, **Na2Mn2**, and **Li2Zn2** were collected at Emory University. Single crystals of all five of these new complexes suitable for X-ray analysis were each coated with Paratone-N oil, suspended in a small fiber loop, and placed in a cooled gas stream on a Brüker D8 SMART APEX CCD sealed tube diffractometer. Diffraction intensities were measured using graphite monochromated Mo Kα radiation (λ = 0.71073 Å) at 173(2) K with a combination of φ and ω scans with 10 s frames, traversing about ω at 0.3° increments. Data collection, indexing, and initial cell refinements were carried out using SMART;[19] frame integration and final cell refinements were done using SAINT.[20] The molecular structure of each complex was determined using direct methods and Fourier techniques and refined by full-matrix least-squares.[21] Multiple absorption corrections, including face indexed absorption correction, were

(19) *SMART, Bruker AXS, I.*; 5.628 ed.; Analytical X-ray Systems: Madison, WI, 2003.

(20) *SAINT, Bruker AXS, I.*; 6.28 ed.; Analytical X-ray Systems: Madison, WI, 2003.

(21) *SHELXTL*; 6.14 ed.; Bruker AXS, Inc.: Madison, WI, 2003.

Table 1. Crystal Data and Structure Refinement for **Na2Co2**, **Na2Ni2**, **Li2Ni2**, **Li2Zn2**, and **Na2Mn2**

	Na2Co2	Na2Ni2	Li2Ni2	Li2Zn2	Na2Mn2
empirical	$H_{56}K_8Na_6Co_2$	$H_{60}K_8Na_6Ni_2$	$H_{26.8}K_3Li_4Ni$	$H_{50}K_6Na_2Li_6$	$H_{46}Na_{14}Mn2$
formula	$O_{96}P_2W_{18}$	$O_{98}P_2W_{18}$	$O_{47.40}PW_9$	$Zn_2O_{93}P_2W_{18}$	$O_{91}P_2W_{18}$
Fw ($g\cdot mol^{-1}$)	5532.53	5507.40	2647.79	5360.70	5258.98
T (K)	173(2)	173(2)	173(2)	173(2)	173(2)
radiation (λ, Å)	0.71073	0.71073	0.71073	0.71073	0.71073
crystal system	triclinic	triclinic	triclinic	triclinic	triclinic
space group	$P\bar{1}$	$P\bar{1}$	$P\bar{1}$	$P\bar{1}$	$P\bar{1}$
a (Å)	11.6790(8)	11.6706(15)	11.550(5)	11.6835(12)	11.442(4)
b (Å)	13.1564(9)	13.1351(16)	13.250(6)	13.1470(13)	12.572(4)
c (Å)	16.3125(11)	16.249(2)	16.056(8)	16.1275(16)	16.438(6)
α (deg)	84.7880(10)	84.778(2)	83.972(7)	84.746(2)	76.545(5)
β (deg)	70.4500(10)	70.453(2)	71.200(7)	70.677(2)	70.883(5)
γ (deg)	68.9890(10)	69.077(2)	67.303(6)	68.127(2)	72.475(5)
V (Å^3)	2203.7(3)	2191.3(5)	2145.5(18)	2168.0(4)	2106.7(12)
Z	1	1	2	1	1
d_{calcd}, $Mg\cdot m^{-3}$	4.126	4.173	4.099	4.069	4.145
μ, mm^{-1}	24.316	24.507	24.897	24.765	24.979
GOF	1.044	1.043	1.004	1.112	1.021
final R indices	$R_1{}^a = 0.0412$,	$R_1{}^a = 0.0347$	$R_1{}^a = 0.0432$	$R_1{}^a = 0.0441$,	$R_1{}^a = 0.0785$,
[$R > 2\sigma(I)$]	$wR_2{}^b = 0.1012$	$wR_2{}^b = 0.0876$	$wR_2{}^b = 0.1143$	$wR_2{}^b = 0.1110$	$wR_2{}^b = 0.2454$
R indices (all data)	$R_1{}^a = 0.0577$,	$R_1{}^a = 0.0439$	$R_1{}^a = 0.0593$	$R_1{}^a = 0.0631$,	$R_1{}^a = 0.1193$,
	$wR_2{}^b = 0.1097$	$wR_2{}^b = 0.0923$	$wR_2{}^b = 0.1246$	$wR_2{}^b = 0.1195$	$wR_2{}^b = 0.2870$

$^a R_1 = \sum||F_0| - |F_c||/\sum|F_0|$. $^b wR_2 = \sum[w(F_0{}^2 - F_c{}^2)^2]/\sum[w(F_0{}^2)^2]^{1/2}$.

applied using the program SADABS.[22] The largest residual electron density for each structure was located close to (less than 1.0 Å from) countercation and tungsten atoms and was most likely due to imperfect absorption corrections frequently encountered in polytungstates and other structures dominated by heavy-metal atoms. All the heavy atoms, including K, Na, Li, P, Co, Ni, Mn, Zn, and W were refined anisotropically. Scattering factors and anomalous dispersion corrections are taken from the International Tables for X-ray Crystallography. Structure solution, refinement, graphics, and generation of publication materials were performed by using SHELXTL, v 6.14, software. Refinement details, structural parameters, selected metal−oxygen bond lengths are summarized in Tables 1 and 2. The corresponding CIF files are available as Supporting Information.

Results and Discussion

Structures. Compounds **Na2M2** and **Li2M2** are isostructural. They consist of two lacunary B-α-$[PW_9O_{34}]^{9-}$ Keggin moieties linked via two M^{2+} ions and two sodium or lithium ions leading to a sandwich-type structure of C_i symmetry (see Figure 1). The central core (belt) of $[M'_2M_2(PW_9O_{34})_2]^{12-}$ complexes is a rhomb-like $M'_2M_2{}^{6+}$ (M = Co, Ni, Mn, Zn) tetragon consisting of two M^{2+} ions located in the two internal positions and two sodium or lithium ions in the external positions. The two transition-metal centers are chemically equivalent and octahedrally coordinated. Each sodium or lithium ion is coordinated to six oxygen atoms of the two B-α-$[PW_9O_{34}]^{9-}$ units. The bond distance of Li to bridging W−O−W oxygen (ca. 2.8−2.9 Å) is longer than the distance of Na to the corresponding bridging W−O−W oxygen (ca. 2.58−2.69 Å). This phenomenon very likely derives from the relative ionic radii of these two alkali metal cations. The trivacant B-α-$PW_9O_{34}{}^{9-}$ anion contains seven unsaturated oxygen atoms, which is very similar to $X_2W_{15}O_{56}{}^{12-}$ (X = P, As). The coordination modes between metal and lacunary POM units in the $[M'_2M_2(PW_9O_{34})_2]^{12-}$ compounds are also very similar to those in the reported Wells−Dawson-derived sandwich-type complexes, $[(NaOH_2)_2(Fe^{III})_2(X_2W_{15}O_{56})_2]^{16-}$ (X = P^V and As^V).[16] The junctions between the two lacunary Keggin fragments with the central unit in the complexes reported here are analogous to the junctions between a particular M_3O_{13} group and to the remainder of the POM structural framework in the parent Keggin and Wells−Dawson polyanions. Specifically, the β isomer for the Keggin derivatives has the M_9 moiety relative to the adjacent unit (the M_3 triad in the case of the parent POMs and the M'_2M_2 unit in the complexes reported here) rotated 60° related to the α isomer. Of all previously known sandwich-type POMs with trivacant B-Keggin units and central M_4 units, most have two β junctions between these units as exemplified in the tetranuclear compounds $[M_4(H_2O)_2(XW_9O_{34})_2]^{n-}$ (X= P^V, Si^{IV}, Ge^{IV}; M = Mn^{2+}, Co^{2+}, Zn^{2+}, Co^{2+} Ni^{2+}), while a few POMs have both α and β junctions as exemplified in

Table 2. Selected Metal−Oxygen Bond Lengths [Å]

Li2Zn2			
Zn(1)−O(31)	2.018(7)	Zn(1)−O(34)	2.036(7)
Zn(1)−O(30)	2.039(7)	Zn(1)−O(33)	2.017(7)
Zn(1)−O(16)	2.206(7)	Zn(1)#7-O(16)	2.220(7)
Na2Co2			
Co(1)−O(30)	2.027(7)	Co(1)−O(31)	2.044(7)
Co(1)−O(34)#1	2.030(7)	Co(1)−O(28)	2.204(7)
Co(1)−O(29)#1	2.039(7)	Co(1)−O(28)#1	2.212(6)
Na2Ni2			
Ni(1)−O(34)#8	2.007(5)	Ni(1)−O(33)#8	2.030(5)
Ni(1)−O(29)	2.008(5)	Ni(1)−O(28)#8	2.165(5)
Ni(1)−O(30)	2.016(5)	Ni(1)−O(28)	2.169(5)
Li2Ni2			
Ni(1)−O(30)	1.989(8)	Ni(1)−O(33)#4	2.019(8)
Ni(1)−O(34)#4	2.008(8)	Ni(1)−O(31)#4	2.139(7)
Ni(1)−O(32)	2.014(7)	Ni(1)−O(31)	2.159(7)
Na2Mn2			
Mn(1)−O(24)#1	2.106(15)	Mn(1)−O(32)	2.098(14)
Mn(1)−O(30)	2.129(15)	Mn(1)−O(34)	2.135(15)
Mn(1)−O(29)	2.282(13)	Mn(1)−O(29)#1	2.293(13)

(22) Sheldrick, G. M. SADABS 2.10, *Bruker AXS I.*, Madison, WI, 2003.

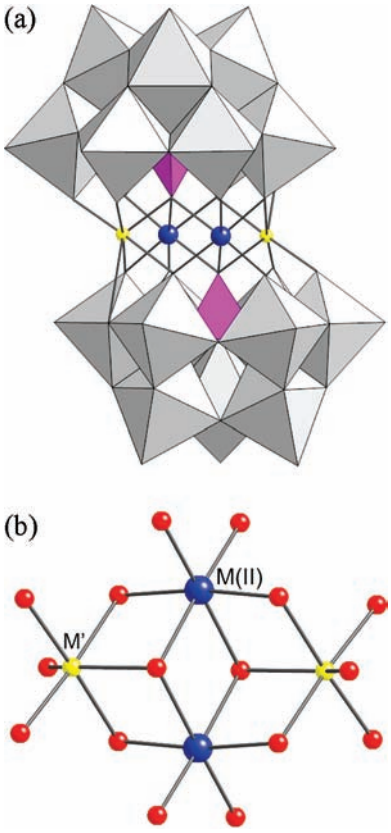

Figure 1. (a) X-ray structure of the polyanions in $[M'_2M_2(PW_9O_{34})_2]^{12-}$. The transition metals and the sodium or lithium are in ball-and-stick notation (transition metals: blue; sodium or lithium: yellow), and the rest of the polyoxometalate framework is in polyhedral notation (WO_6 octahedra: gray, PO_4 tetrahedron: pink). Hydrogen atoms are omitted for clarity. (b) The connection motif of the metal atoms between the two B-α-$PW_9O_{34}^{9-}$ units (M: transition metal; M′: sodium or lithium).

the trimetal-containing POM $[Ni_3Na(H_2O)_2(XW_9O_{34})_2]^{11-}$ ($X = P^V$, As^V).[13] The $[M'_2M_2(PW_9O_{34})_2]^{12-}$ complexes in this paper have two α junctions between the trivacant POM units and the central $M_2M'_2$ unit. This is as same interunit isomerism seen in $[(NaOH_2)_2(Fe^{III})_2(X_2W_{15}O_{56})_2]^{16-}$,[16] namely αααα. Such interunit isomerism has not heretofore been seen in the Keggin-based POMs.

Relatively few sandwich-type POMs based on trivacant Keggin units contain two transition metals in the belt, and all known examples are based on A-type Keggin POM units (A-$PW_9O_{34}^{9-}$, A-$GeW_9O_{34}^{10-}$, A-$SiW_9O_{34}^{10-}$, $Sb^{III}W_9O_{33}^{9-}$, $Te^{IV}W_9O_{33}^{8-}$)[17] and actinyl species UO_2^{2+} and NpO_2^{2+}. In the actinyl polyoxoanions formed from A-$XW_9O_{34}^{n-}$, the UO_2^{2+} and NpO_2^{2+} moieties are in the external positions, and each bear one terminally ligated aqua ligand, while two sodium ions reside in the internal positions. In contrast, there are no sodium ions in the central belt in the diuranium sandwich-type POMs based on $Sb^{III}W_9O_{33}^{9-}$ and $Te^{IV}W_9O_{33}^{8-}$, and the two uranium centers are seven coordinate with three terminal aqua ligands each. Xu's group reported the X-ray structure of three complexes that contain the trivacant unit, $[As^VMo_9O_{33}]^{7-}$, namely $[Mn_2(As^VMo_9O_{33})_2]^{10-}$, which is a monomeric, and $[Mn_2(As^VMo_9O_{33})_2]^{10-}$ or $[Co_2(As^VMo_9O_{33})_2]^{10-}$ which are polymeric (one-dimensional structures). The common structural component, $[As^VMo_9O_{33}]^{7-}$, is a derivative of the B-β trivacant Keggin unit. To the best of our knowledge, sandwich POMs with two transition metals in the belt that we report here, $[M'_2M_2(PW_9O_{34})_2]^{12-}$, represent a new family of POMs based on the B-α Keggin trivacant polyanion.

IR Characterization. The infrared spectra of these POMs in the P−O, W−O, and W−O−W stretch regions are very similar to each other strongly suggesting that these complexes are isostructural to one another (see Supporting Information, Figures S1 and S2). The ν_3 vibrational mode of the central PO_4 unit in these compounds is split, indicating a structural distortion and a consequent lowering of the symmetry around these central units. The peaks in the low energy (< 1000 cm^{-1}) region are attributed to the characteristic $\nu(W-O_d)$, $\nu(W-O_b-W)$ and $\nu(W-O_c-W)$ absorptions, where O_b = double-bridging oxygen; O_c = central oxygen; and O_d = terminal oxygen.

^{31}P NMR Characterization. ^{31}P NMR spectroscopy is a very useful technique to address the purity and stability of polytungstophosphates. ^{31}P NMR spectra of the $[M'_2M_2(PW_9O_{34})_2]^{12-}$ complexes in D_2O or 1 M LiCl/D_2O solution in a low-frequency region at room temperature show that the $[M'_2M_2(PW_9O_{34})_2]^{12-}$ complexes dissociate to d-electron transition-metal ions, M, and B-α-$PW_9O_{34}^{9-}$; the latter further decomposes to $PW_{11}O_{39}^{7-}$ and PO_4^{3-} (see Supporting Information, Figure S3). The ^{31}P NMR spectra for **M′2Co2**, **M′2Ni2**, and **M′2Zn2** in D_2O at 277, 286, and 296 K (before decomposition products can be detected) are reported in Figures 2 and 3, and all data are given in Table 3. The chemical shifts of **Na2Co2**, **Li2Co2**, **Na2Ni2**, and **Li2Ni2** increase with decreasing temperature, while those of **Na2Zn2** and **Li2Zn2** are fairly temperature independent (Figure 4). No signal is observed for **Na2Mn2** and **Li2Mn2** in the high-frequency region because of the strong influence of the $S = 5/2$ Mn(II) centers on ^{31}P nuclear relaxation rates.

Since the solubility of $[M'_2M_2(PW_9O_{34})_2]^{12-}$ in D_2O is much lower than in 1 M LiCl, we choose to study the decomposition of **Li2M2** in 1 M LiCl.[23] The ^{31}P NMR spectrum of **Li2Zn2** in 1 M LiCl obtained immediately after mixing shows a single peak at −3.6 ppm. After 1 day, a new peak at -4.1 ± 0.1 ppm attributable to the $[Zn_4(H_2O)(PW_9O_{34})_2]^{10-}$ (Supporting Information, Figure S4) forms in addition to peaks for PO_4^{3-} and $PW_{11}O_{39}^{7-}$. The ^{31}P NMR spectra for the paramagnetic compounds, **Li2Co2** and **Li2Ni2**, in 1 M LiCl exhibit one line at ca. 1464 and 1117 ppm (Supporting Information, Figure S5 and S6) respectively, consistent with two equivalent $PW_9O_{34}^{9-}$ moieties in both cases. After 6 days, no additional peaks are observed in the spectrum of **Li2Ni2**, indicating no other species form in the solution (Supporting Information, Figure S7). The solution of **Li2Co2** shows the generation of $Co_4(H_2O)_2(PW_9O_{34})_2^{10-}$ and other species after several days (Supporting Information, Figure S8). $[Co_3Na(H_2O)_2(XW_9O_{34})_2]^{11-}$ could well be one of these

(23) Experimental conditions for paramagnetic **Li2Co2** and **Li2Ni2** in 1 M LiCl at 296 K: Varian INOVA 400 spectrometer, spectral width: 400 kHz; pulse width: 6 μs; number of points: 18 816; acquisition time: 24 ms for **Li2Co2** and 12 ms for **Li2Ni2**; line broadening factor: 100 Hz for **Li2Co2** and 400 Hz for **Li2Ni2**. Experimental conditions for diamagnetic **Li2Zn2**: Varian INOVA 400 spectrometer, spectral width: 20 kHz; pulse width: 13 μs; number of points: 48 000; acquisition time: 1.2 s; line broadening factor: 3 Hz.

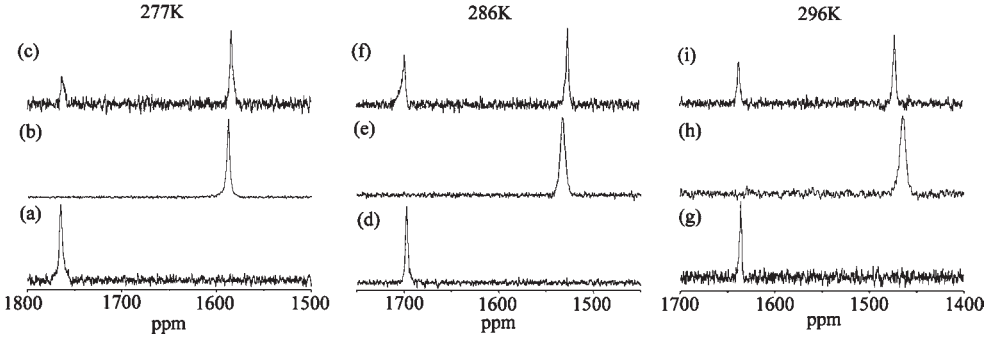

Figure 2. ^{31}P NMR spectra of aqueous solutions of (a) **Na2Co2**, (b) **Li2Co2**, and (c) **Na2Co2** (in the presence of 2.8 mM LiCl) at 277 K; (d) **Na2Co2**, (e) **Li2Co2**, and (f) **Na2Co2** (in the presence of 2.8 mM LiCl) at 286 K; and (g) **Na2Co2**, (h) **Li2Co2**, and (i) **Na2Co2** (in the presence of 2.8 mM LiCl) at 296 K.

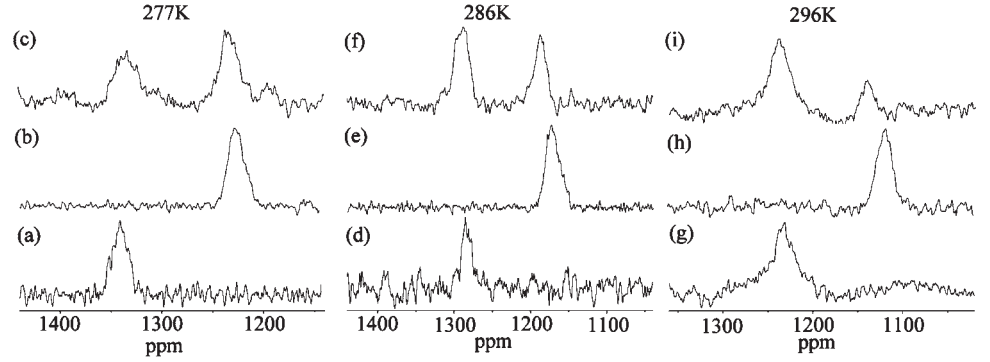

Figure 3. ^{31}P NMR spectra of aqueous solutions of (a) **Na2Ni2**, (b) **Li2Ni2**, and (c) **Na2Ni2** (in the presence of 2.8 mM LiCl) at 277 K; (d) **Na2Ni2**, (e) **Li2Ni2**, and (f) **Na2Ni2** (in the presence of 2.8 mM LiCl) at 286 K; and (g) **Na2Ni2**, (h) **Li2Ni2**, and (i) **Na2Ni2** (in the presence of 2.8 mM LiCl) at 296 K.

Table 3. ^{31}P NMR data for the $[M'_2M_2(PW_9O_{34})_2]^{12-}$ Complexes[a]

compound	277 K δ (ppm)	286 K δ (ppm)	296 K δ (ppm)
Na2Co2	1764	1697	1635
Li2Co2	1588	1532	1464
Na2Ni2	1341	1284	1231
Li2Ni2	1222	1173	1117
Na2Zn2	−2.5	−2.4	−2.2
Li2Zn2	−3.9	−3.7	−3.6

[a] Experimental conditions for paramagnetic **Na2Co2**, **Li2Co2**, **Na2Ni2**, and **Li2Ni2**: Unity Plus 600 spectrometer, spectral width: 100 kHz; pulse width: 4 μs (~40° flip angle); number of points: 4800; acquisition time: 24 ms; line broadening factor: 100 Hz for **Na2Co2** and **Li2Co2** and 400 Hz for **Na2Ni2** and **Li2Ni2**. Experimental conditions for diamagnetic **Na2Zn2** and **Li2Zn2**: Unity Plus 600 spectrometer, spectral width: ~32 kHz; pulse width: 8 μs; number of points: 63 898; acquisition time: 1s; line broadening factor: 3 Hz.

other decomposition products; the isostructural nickel analogue is known.[13] $CoPW_{11}O_{39}^{5-}$ (448 ppm) could well be an intermediate, but it is not observed. When $Li_2Co_2(H_2O)_2(PW_9O_{34})_2^{12-}$ or $Li_2Zn_2(H_2O)_2(PW_9O_{34})_2^{12-}$ dissociate, free $PW_9O_{34}^{9-}$ units prefer to bind the metals first to form sandwich-type structures, then the unreacted $PW_9O_{34}^{9-}$ left in the solution subsequently decomposes to $PW_{11}O_{39}^{7-}$ and PO_4^{3-}. The relative rates of metal−cation exchange reactions correlate with the ligand field stabilization energies of the central transition metals in the belt of these sandwhich POMs: **Li2Zn2** (most reactive; ligand-field stabilization energy, LFSE = 0) > **Li2Co2** (LFSE = $0.8\Delta_o$) > **Li2Ni2** (least reactive; LFSE = $1.2\Delta_o$).

Addition of 10 μL of 0.2 M LiCl/D_2O solution to aqueous solutions of **Na2Co2** and **Na2Ni2** (final LiCl concentration ~2.8 mM) at different temperatures (277, 286, and 296 K) results in a new peak that corresponds to a new species (Figures 2c, f, i and 3c, f, i). The chemical shifts of the new species are similar to those of the **Li2Co2** and **Li2Ni2**, which indicate that a lithium−sodium exchange has taken place in solution. In fact, lithium−sodium exchange has also been confirmed by X-ray crystallography. Lithium−sodium exchange is also seen for solutions of **Na2Zn2**, but fast decomposition of this complex renders the spectral quality poor due to the short data-acquisition time.

Time profiles of electronic absorption spectra of **Li2M2** in 1 M LiCl have also been obtained (Supporting Information, Figure S9−S12), and they clearly reveal the decay of these compounds in solution. The decomposition kinetics in all cases do not obey any simple rate law.

Magnetic Susceptibility. The temperature dependence of magnetic susceptibility χ_m for **Na2Co2**, **Na2Ni2**, and **Na2Mn2** was investigated in the range of 2−300 K with an applied field of 1000 Oe. The $\chi_m T$ product versus T for **Na2Co2** is shown in Figure 5. Since Co(II) ion has a $^4T_1$ high-spin ground state in an octahedral environment, the significant orbital contribution results in a deviation of the room temperature-effective magnetic moment per Co_2 unit (6.38 emu K mol^{-1}) from the expected spin-only value for two Co(II) ions ($S = 3/2$, $g = 2.0$).[24] Upon cooling from room temperature, the $\chi_m T$ value decreases continuously until it reaches a minimum of 5.03 emu K mol^{-1} at 30 K. Such a decrease is due to strong spin−orbit coupling of Co(II) ion, from which six Kramers doublets result. Below 30 K, the $\chi_m T$ value increases abruptly to a maximum of 5.78 emu K mol^{-1} at 6 K. Taking into

(24) Carlin, R. L.; Van Duyneveldt, A. L. *Magnetic Properties of Transition Metal Compounds*; Springer-Verlag: New York, 1977; pp 69.

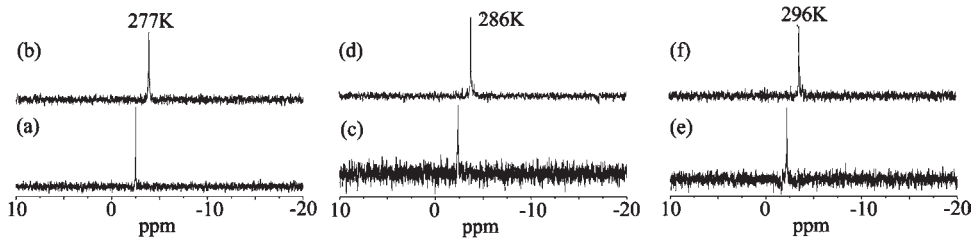

Figure 4. ^{31}P NMR spectra of (a) **Na2Zn2** and (b) **Li2Zn2** in D_2O at 277 K; (c) **Na2Zn2** and (d) **Li2Zn2** in D_2O at 286 K; and (e) **Na2Zn2** and (f) **Li2Zn2** in D_2O at 296 K.

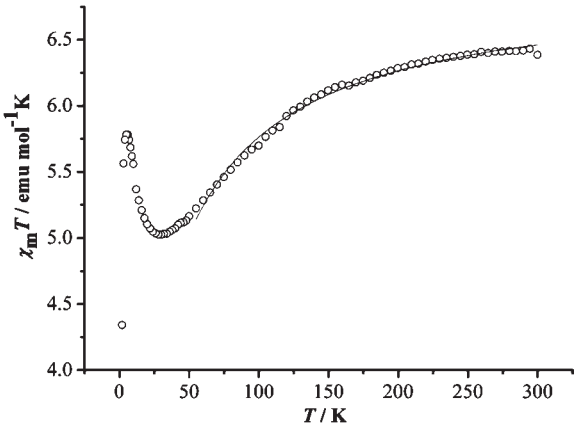

Figure 5. Temperature dependence of $\chi_m T$ for **Na2Co2**. The solid lines correspond to the best-fit curves using the parameters described in the text.

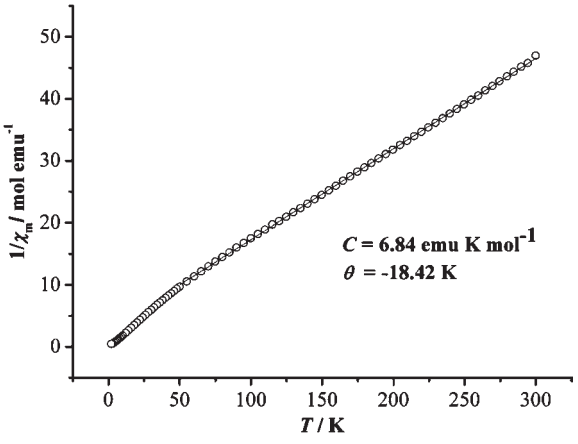

Figure 6. Temperature dependence of $1/\chi_m$ for **Na2Co2**. The solid line is the best fit.

account the orthogonality of the magnetic orbitals in the Co_2O_{10} unit, the increase of $\chi_m T$ should be indicative of ferromagnetic interactions in the Co(II)−Co(II) dinuclear entities. Then, the $\chi_m T$ value decreases again to 4.34 emu K mol^{-1} at 2 K; this is attributed to that the fact that the d electrons only populate the lowest Kramers doublet at very low temperature. The susceptibility data (see in Figure 6) for **Na2Co2** can be fit with the Curie−Weiss equation from 25 to 300 K, giving $C = 6.84$ emu K mol^{-1} and $\theta = -18.42$ K. To simplify the model, the Heisenberg spin-coupled Hamiltonian $\hat{H} = -2J\hat{S}_1 \cdot \hat{S}_2$ was applied to simulate the susceptibility data above 50 K, where J is the intradimer interaction parameter between the Co(II) ions; a Weiss constant was introduced as well. The best-fit parameters obtained are $J = 4.90$ cm^{-1}, $g = 2.71$, $\theta = -30.23$ K, and $R = 9.1 \times 10^{-4}$ (the error factor R is defined as $\sum[(\chi_m T)_{obs} - (\chi_m T)_{calc}]^2/\sum[(\chi_m T)_{obs}^2]$). The J value is comparable to those of previously reported cobalt compounds.[25,26]

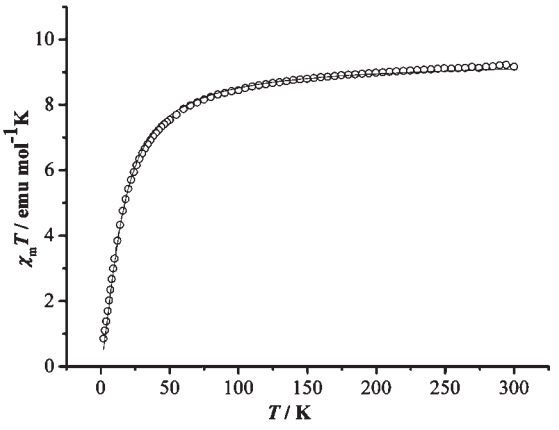

Figure 7. Temperature dependence of $\chi_m T$ for **Na2Mn2**. The solid line corresponds to the best-fit curve using the parameters described in the text.

The magnetic properties of **Na2Mn2** in the form of a $\chi_m T$ versus T plot are shown in Figure 7. The $\chi_m T$ value stays basically at 9.16 emu K mol^{-1} from room temperature down to about 100 K, close to the expected value (8.75 emu K mol^{-1}) for two isolated spin-only Mn(II) center ($s = 5/2$, $g = 2.0$) in an octahedral field. Below 50 K, the $\chi_m T$ value suddenly drops down to 0.85 emu K mol^{-1} at 2 K, consistent with an antiferromagnetic interaction in the Mn(II)−Mn(II) dinuclear units. The $1/\chi_m$ versus T plot (see in Figure 8) for **Na2Mn2** could be fit with the Curie−Weiss equation from 25 to 300 K, producing $C = 9.61$ emu K mol^{-1} and $\theta = -13.84$ K, the negative Weiss constant indicating the occurrence of a dominant antiferromagnetic interaction between the neighboring Mn(II) atoms. The experimental data could be fitted to a Heisenberg spin Hamiltonian ($S_1 = S_2 = 5/2$) spin-coupled model assuming $\hat{H} = -2J\hat{S}_1 \cdot \hat{S}_2$, where J is the intradimer interaction parameter between the Mn(II) ions. By using least-squares methods, a satisfactory fit of the data was obtained with parameters, $J = -1.09$ cm^{-1} and $g = 2.07$. The agreement factor $R = \sum(\chi_m T_{obs} - \chi_m T_{calc})^2/\sum(\chi_m T_{obs})^2$ is 1.0×10^{-4}. The J value is similar to that found in other manganese polyoxotungstate compounds.[27] The results indicate the

(25) Bassil, B. S.; Nellutla, S.; Kortz, U.; Stowe, A. C.; van Tol, J.; Dalal, N. S.; Keita, B.; Nadjo, L. *Inorg. Chem.* **2005**, *44*, 2659.
(26) Galán-Mascarós, J. R.; Gómez-García, C. J.; Borrás-Almenar, J. J.; Coronado, E. *Adv. Mater.* **1994**, *6*, 221.
(27) Gómez-García, C. J.; Coronado, E.; Gómez-Romero, P.; Casañ-Pastor, N. *Inorg. Chem.* **1993**, *32*, 3378.

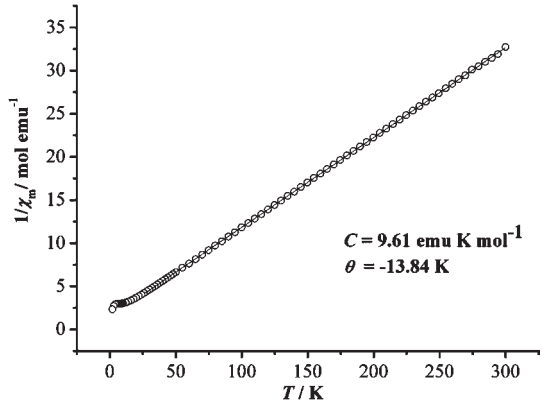

Figure 8. Temperature dependence of $1/\chi_m$ for **Na2Mn2**. The solid line is the best fit.

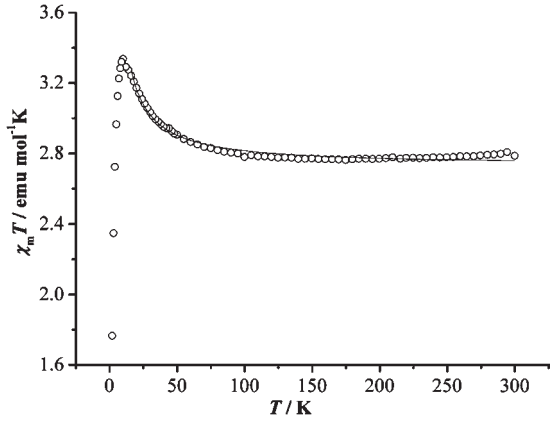

Figure 9. Temperature dependence of $\chi_m T$ for **Na2Ni2**. The solid lines correspond to the best-fit curves using the parameters described in the text.

presence of a weak antiferromagnetic interaction between the neighboring Mn(II) centers within the cluster.

The magnetic properties of **Na2Ni2** were measured over the range 2−300 K and are shown in Figure 9. The experimental $\chi_m T$ values of **Na2Ni2** at room temperature are 2.78 emu K mol^{-1} per formula, which is larger than that expected for the total spin-only value for two Ni^{2+} ions (s = 2, g = 2.0). The $\chi_m T$ values increase from ambient temperature down to 10 K with a maximum of 3.34 emu K mol^{-1}, then decreasing sharply to 1.76 emu K mol^{-1} at 2 K. The increase of $\chi_m T$ indicates the presence of noticeable ferromagnetic interactions within the dinuclear entities, and the low-temperature drop may be attributed to secondary effects, such as zero-field splitting (ZFS) and/or intermolecular antiferromagnetic interactions. The temperature dependence of the reciprocal susceptibilities ($1/\chi_m$) obeys the Curie−Weiss law with C = 2.76 emu K mol^{-1} and θ = 1.53 K (Figure 10), which supports the presence of overall ferromagnetic coupling between the Ni^{2+} ions. To analyze the observed magnetic behavior, the isotropic exchange Hamiltonian $\hat{H} = -2J\hat{S}_1 \cdot \hat{S}_2$ was used for **Na2Ni2**, where J is the intradimer interaction parameter between Ni(II) ions; a Weiss constant was also introduced. The best parameters from

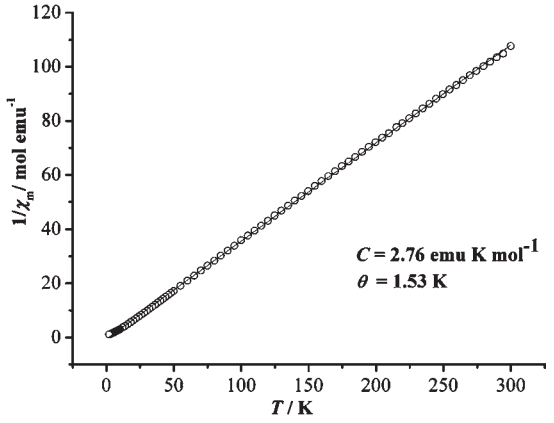

Figure 10. Temperature dependence of $1/\chi_m$ for **Na2Ni2**. The solid line is the best fit.

fitting the data from 15 to 300 K are J = 2.27 cm^{-1}, g = 2.08, C = 1.64 emu K mol^{-1}, θ = 2.41 K and R = 3.6×10^{-4} (the error factor R is defined as $\sum[(\chi_m T)_{obs} - (\chi_m T)_{calc}]^2/\sum[(\chi_m T)_{obs}^2]$). The J value is in agreement with that of other reported Ni polyoxotungstates.[28] The results confirm that the Ni···Ni interactions are ferromagnetic.

Conclusions

We have prepared a series of sandwich-type polytungstophosphates in which two different types of metals are sandwiched between two B-α-$PW_9O_{34}^{9-}$ units. All these polyanions have been fully characterized by FTIR, elemental analysis, and solution ^{31}P NMR spectroscopy. Compounds **Na2Co2**, **Na2Ni2**, **Li2Ni2**, **Na2Mn2**, and **Li2Zn2** have been characterized by single crystal X-ray diffraction. The stabilities of all these compounds have been studied by solution ^{31}P NMR spectroscopy. None of these compounds are stable in aqueous solution; all will dissociate into metal ions and $PW_9O_{34}^{9-}$. The latter ultimately transforms into $PW_{11}O_{39}^{7-}$ and PO_4^{3-}. **Li2Co2** and **Li2Zn2** convert primarily into the sandwich-type POMs with four transition metals in the belt; whereas, **Li2Ni2** slowly decomposes into a mixture of polytungstates but no Ni-containing POMs. An investigation of the magnetic properties of **Na2Co2**, **Na2Ni2**, and **Na2Mn2** indicates that the exchange interactions within the dinuclear units are ferromagnetic in **Na2Co2** (at 6−30 K) and in **Na2Ni2** (2−300 K). However, **Na2Mn2** exhibits an antiferromagnetic interaction between the two Mn^{2+} ions at 2−50 K.

Acknowledgment. C.L.H. thanks the Defense Treat Research Agency (grant no. HDTRA1-09-1-0002), and L.X. thanks the National Natural Science Foundation of China (grant no. 20731002) for support of this research.

Supporting Information Available: Infrared, ^{31}P NMR spectra, and time profile of electronic absorption spectra of **Li2M2** of these new sandwich-type POMs. This material is available free of charge via the Internet at http://pubs.acs.org.

(28) Mbomekalle, I. M.; Keita, B.; Nierlich, M.; Kortz, U.; Berthet, P.; Nadjo, L. *Inorg. Chem.* **2003**, *42*, 5143.